Presented at IPC Printed Circuits Expo®
SMEMA Council APEX®
Designers Summit 04

Dynamic Testing and Modeling for Solder Joint Reliability Evaluation

Phil Geng
Intel Corporation
Hillsboro, OR

James F. Maguire
Intel Corporation
Dupont, WA

Abstract
The behavior of BGA solder joints under dynamic loads has become more significant in recent years. This work explored test methodologies for solder joint failure evaluation under dynamic loads. The objectives of this study were

- To evaluate the behavior of solder joints under a variety of strain rates as seen during both 4 point bend testing and mechanical shock
- To try to quantify the shock levels present at solder joint failure to support ongoing solder joint reliability modeling efforts

A test coupon and fixture developed for the four point bend test setup is reviewed. Testing was performed under different strain rates and the results showed clearly that the solder joint failure is strongly strain rate dependent under mechanical bending load on boards. This implies that the practice of low strain rate (quasi-static) test with dynamic amplification factor for solder joint failures, such as the four point bend test, is not sufficient for dynamic prediction due to over-estimation of the joint strength at low strain rate range. The finite element analysis revealed that the strain rate dependent material properties of the solder play the key role of solder joint failure threshold.

Comparison of strain rates between the four point bend test and a more traditional mechanical shock test were made on a desktop motherboard. These tests showed that the strain rate is much higher during the mechanical shock test than that seen during the bend testing. A variable mass shock test and an incremental shock test procedure were developed to evaluate BGA solder joint shock failures. In-situ solder joint continuity was monitored during the shock events. The results of these tests give a good estimate of motherboard BGA solder joint robustness.

In addition, a shock test fixture and a test vehicle were developed similar to those used in the four point bend test. By using the incremental shock test procedure outlined above, the acceleration level (G-level) at solder joint failure was obtained. This information was input to the finite element dynamic analysis, the overall behavior of the test coupon during shock was simulated and the solder joint failure force obtained. Failure analysis of the shocked boards revealed that PCB pad/FR4 disbond was the dominant failure mode for the tested eutectic solder joints. In addition, fracture at IMC between pad and solder on the package side was observed.

In summary, a set of test and modeling methodology for solder joint reliability evaluation under dynamic load was developed and validated and some recommendations are made as to the applicability of these test methods.

Introduction
The behavior of BGA solder joints under dynamic loads has become more significant[1,2] due to various issues related to: (i) the occurrence of brittle solder joint failures (e.g. "black pad"), (ii) heavier heat sinks required for new, higher speed micro-processors, (iii) the more severe usage conditions seen in hand held devices and laptop computers.

Research related to strain rate effect on solder joint failure has been gaining more attention recently. Shi, et al[3] performed the tensile test and found that Young's modulus of 63Sn/37Pb solder increases quite linearly with strain rate. Yield stress and ultimate tensile strength show non-linear relationships with strain rate. Both properties increase significantly at low strain rate range (< 0.02/sec) and stay approximately constant at higher strain rate range (>0.02/sec). Dai and Lee[4] tested 63Sn/37Pb solder using punch shear test specimen under static load and impact load. They found adiabatic shear localization at the solder joint under impact load and the dynamic shear strength was more than double the static one.

Geng, et al[5] examined the strain rate effect of BGA solder joint failure on PCB under flexural bend loads on printed circuit boards. A test coupon and fixture was developed for the four-point bend test setup, as shown in Figure 1 and Figure 2. The test is designed to evaluate solder joint failures of BGA/PCB interconnects under flexural load, which is the typical usage condition under mechanical loads.

Testing was performed under different cross-head speeds, which correspond to different strain rates. The strain gages used in this work measured uni-axial strain along the long edge direction of the test coupon. Strain and strain rate values were monitored near the corner of BGA substrate on PCB surface, as shown in Figure 3.

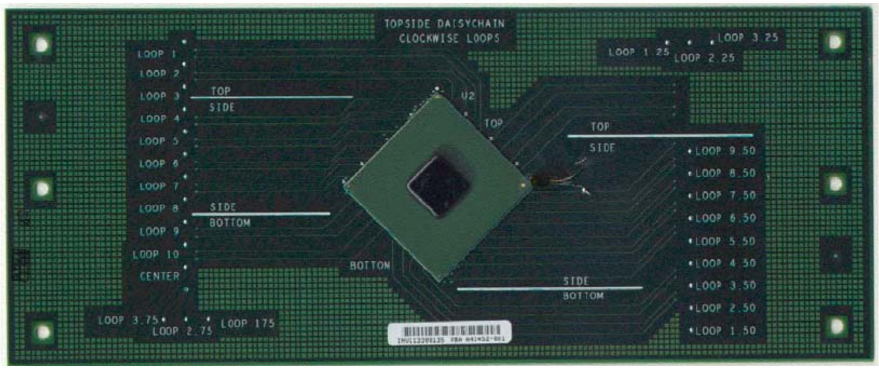

Figure 1 – Test Coupon

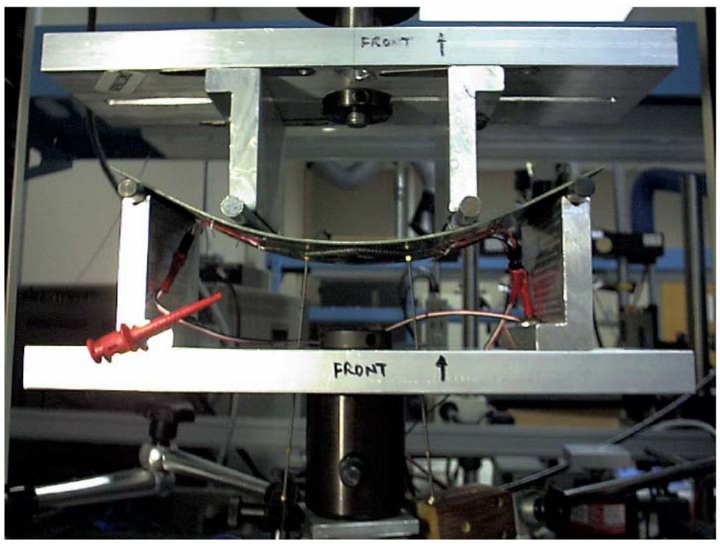

Figure 2 – Four-Point Bend Test Fixture and Setup

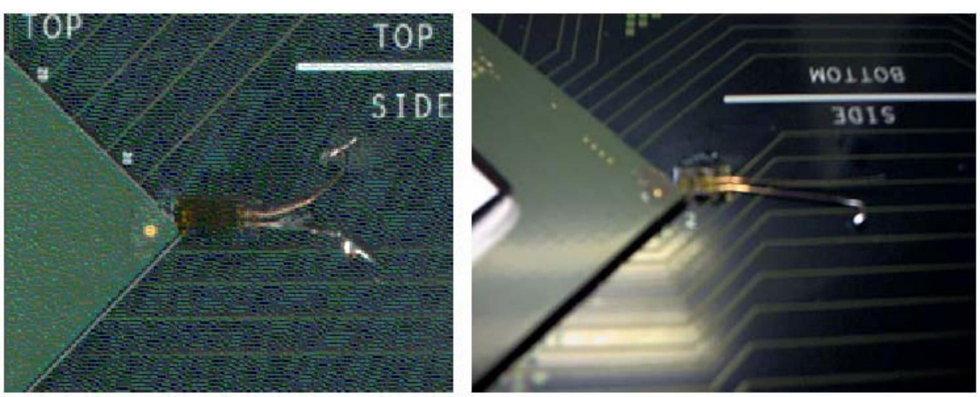

Figure 3 – Strain Gage Monitoring

Strain Rate Effect on Healthy Solder Joints

The load deflection (Figure 4) curves of a 37.5 mm BGA with 1.27 mm pitch and eutectic solder joints are shown in Figure 5. The results showed that under higher loading speed (i.e. higher strain rate), the board deflection and load are lower when solder joints failed (end of each curve in the figure). Under dynamic (shock) load, the board load-deflection point at solder joint failure is not known. From the trend of this data, it is possible that shock failure level is even lower in the range shown in Figure 5.

Figure 6 extracts the failure deflections of 37.5mm BGA with 1.27mm pitch and eutectic solder joints in Figure 5 and shows clearly that the solder joint failure is strongly strain rate dependent under mechanical load. While the trend at higher shock strain rate is not provided, this test demonstrated that the practice of low strain rate (quasi-static) test for solder joint failures with a dynamic amplification factor is not sufficient for dynamic failure prediction due to over-estimation of the joint strength at the low strain rate.

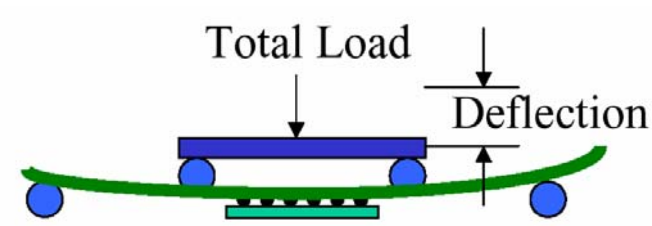

Figure 4 – Load and Deflection Measurement

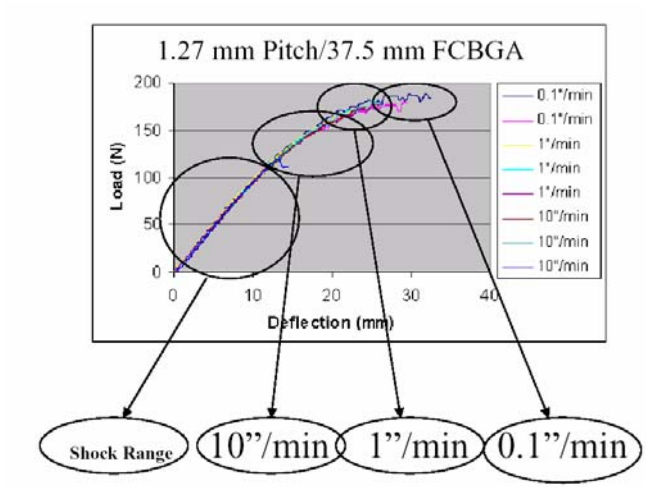

Figure 5 – Load-Deflection Curves Indicating Region of Solder Joint Failure at Various Strain Rates

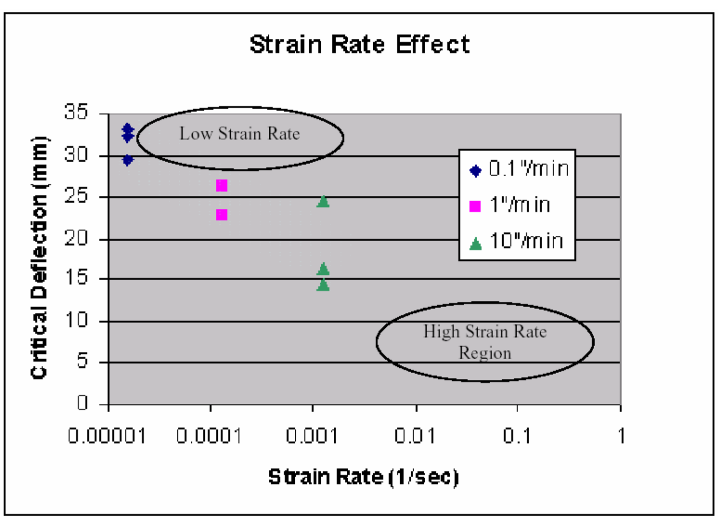

Figure 6 – Strain Rate Effect on Critical Board Deflection of Healthy Solder Failure (37.5 mm BGA with 1.27 mm Pitch and Eutectic Solder Joints)

The finite element analysis (FEA, Figure 7) was performed with different material properties corresponding to the different strain rates of the bend tests. A quarter of the model is shown in Figure 7. The solder joint was simulated with non-linear perfect plastic model and the rest of the materials with elastic model. The PCB board bending was simulated with geometric non-linearity for the large deformation. The support and the loading spans were simulated with the contact element.

The solder joint fracture is not included in the model. The numerical simulation went beyond the solder joint failure points until the edge of the board slips out of the supporting span. The numerical data agrees well with the global bend test data, as shown in Figure 8.

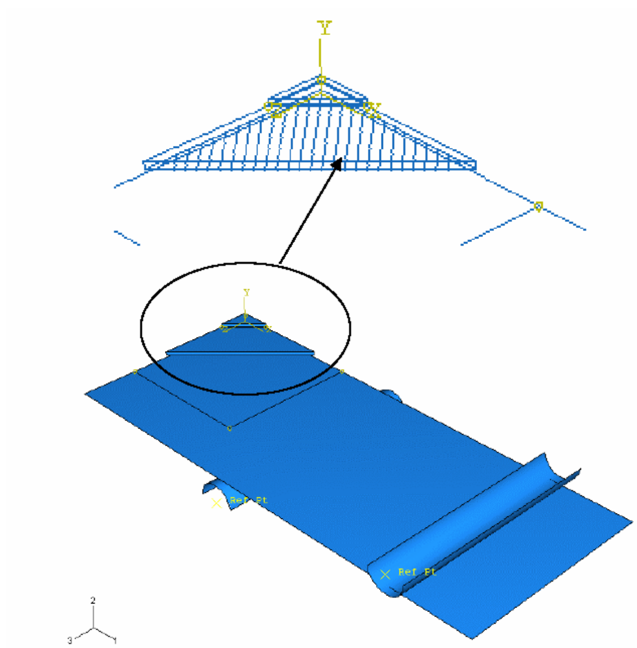

Figure 7 – Four-Point Bend Finite Element Model (1/4 Model with 1.27 mm Pitch/37.5 mm BGA)

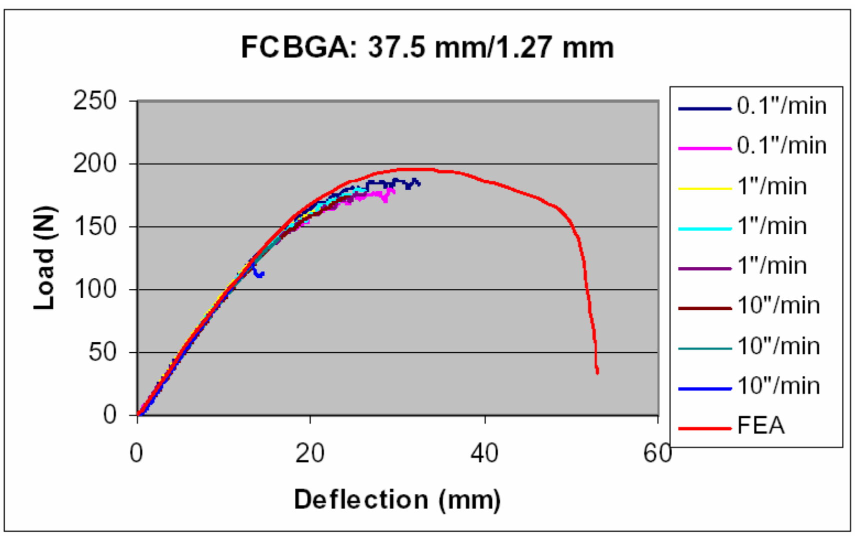

Figure 8 – Comparison of Four-Point Bend FEA Simulating and Test Curves

Figure 10 shows that the strain rate dependent Young's modulus and yield strength of the solder play the key role of solder joint failure threshold. The corner joint examined is show in Figure 9. Strain rates corresponding to different board displacements and the corner joint loads are highlighted. Significant plasticity (and creep not considered in the model) is observed in the FEA model due to the absence of the fracture.

For high strain rate range (green area), the solder yielding and plasticity may not be significant during solder joint failure with the brittle failure and possibly limited plastic deformation.

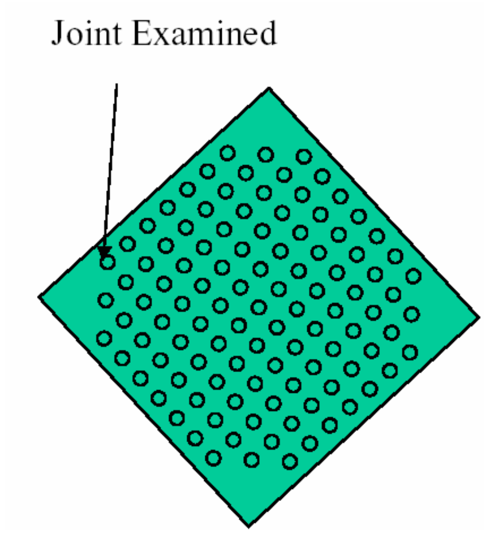

Figure 9 – Corner Joint Examined in Figure 10

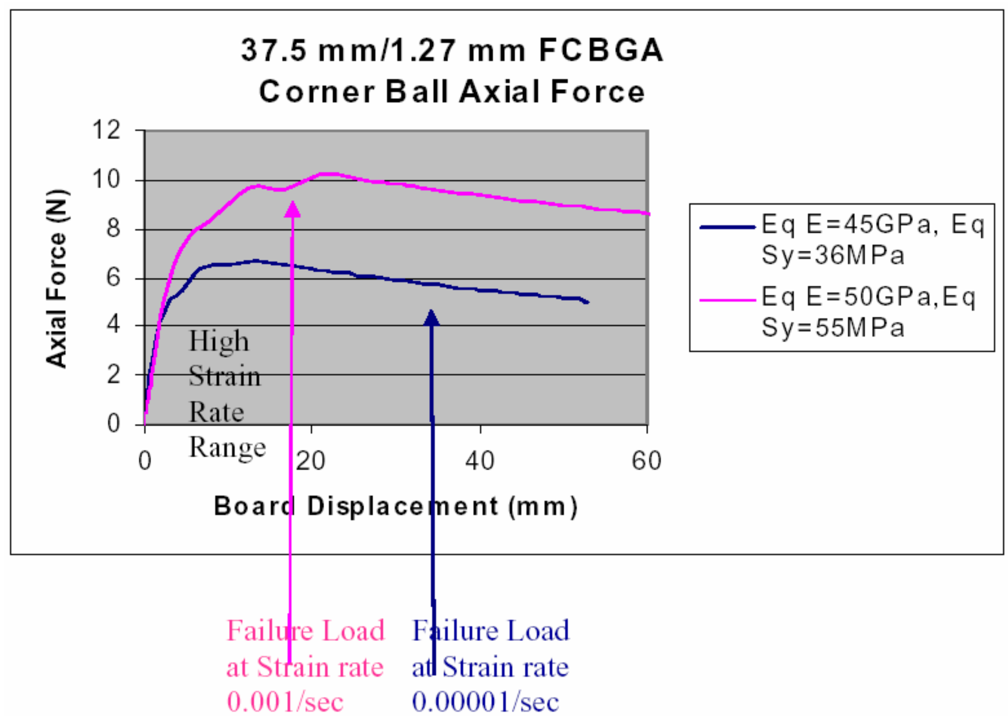

Figure 10 – FEA Simulation of Strain Rate Effect on Solder Joint Axial Forces at BGA Corner Joint during Four-Point Bend Test

Strain Rate Effect on Brittle Solder Joints

The data shown (Figure 6) demonstrates strain rate dependent phenomenon of good healthy solder joints. With the brittle solder joints observed by Goyal, et al.[6] in a 1.0 mm pitch BGA package (due to Electroless Nickel Immersion Gold – ENIG on the package side IMC), same four-point bend test was performed to evaluate potential solder joint embrittlement effects. The board deflections are much lower and the strain rate effect is less, as shown in Figure 11. This brittle effect with relatively less strain rate dependency is later confirmed at the high strain rate[7] by Harada, et al. The lower board deflection at failure and the insensitive strain rate dependency can be good indicators of solder joint brittle failure.

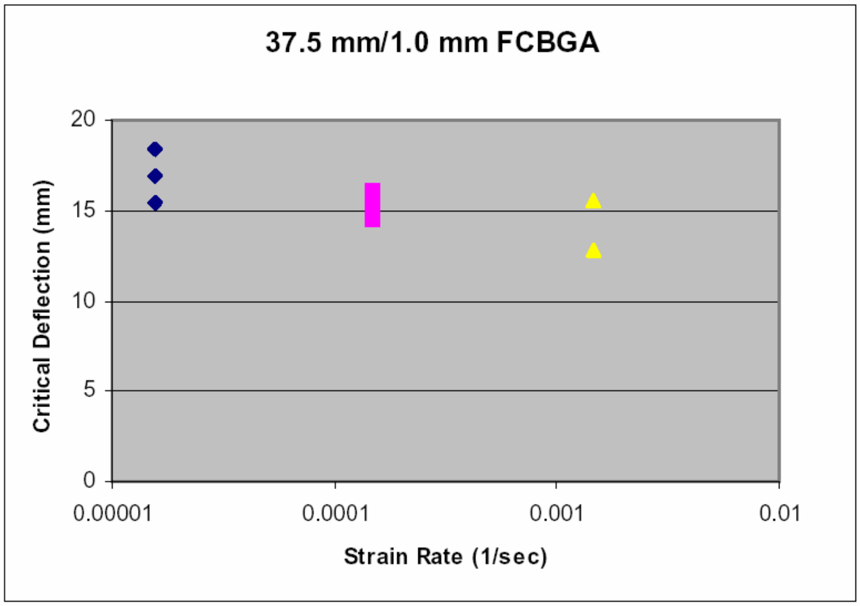

Figure 11 – Strain Rate Effect on Critical Board Deflection of Brittle Solder Failure (37.5 mm BGA with 1.0 mm Pitch and Eutectic Solder Joints

Estimation of Strain Rate Range under Dynamic Load

Under realistic dynamic usage conditions, the strain varies in a range because of the oscillatory response of electronic systems. Therefore, strain rates (derivative of strains) also vary in oscillatory nature during a shock event. In order to evaluate the strain rate range, a desktop computer chassis with a motherboard was tested[8] under shock load, as shown in Figure 12.

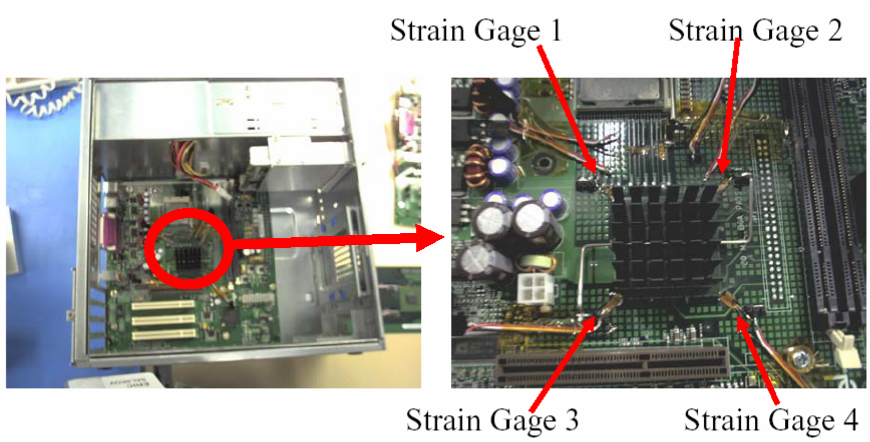

Figure 12 – Shock Test with a Motherboard into a Computer Box

A 30 G acceleration shock load with trapezoidal pulse shape and 4.3 m/sec velocity change was applied. Strain gages were mounted at the 4 corners of the BGA on the PCB boards. In this early study, uni-axial strain gages were used (same gages as the four-point bend tests) and the orientation of strain gages is 135 degree from both BGA edges. With the adoption of rosette, the orientation of strain gage is critical and complete in-plane strain information can be obtained.

The motherboard in the system is facing downward (-Z direction) during the shock test, which corresponds to the worst case from the strain measurement. The data was taken with an oscilloscope to avoid any sampling rate issue. The strain histories during the shock event are plotted in Figure 13. The strain measurement provided the relative BGA solder joint strains and stresses at the four corners, with the BGA corner at the strain gage 2 experiencing the highest strain during the shock event.

The finite element analysis of the strain response at the same BGA corner locations were performed, as shown in Figure 14. For the maximum strain at the location of strain gage 2, the response of the tested and simulated data validated each other quite well.

With the highest strain response at strain gage #2, Figure 15 shows the approximate linear strain rate estimation of the oscillating curves at 0.67/sec by slope fitting. Comparison of strain rates between the low strain rate (quasi-static bend) test (0.00001~0.001/sec, Figure 6) and a more traditional high strain rate (mechanical shock) test (~0.67/sec, Figure 15) showed that the strain rate is much higher during a mechanical drop test than that seen during the bend testing. Therefore, dynamic test is necessary to address both strain rate variation during shock tests and the oscillatory fatigue effect.

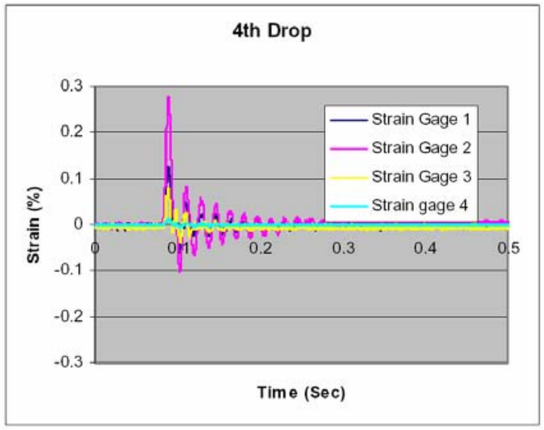

Figure 13 – Strain Response at Four BGA Corners during One Shock Event

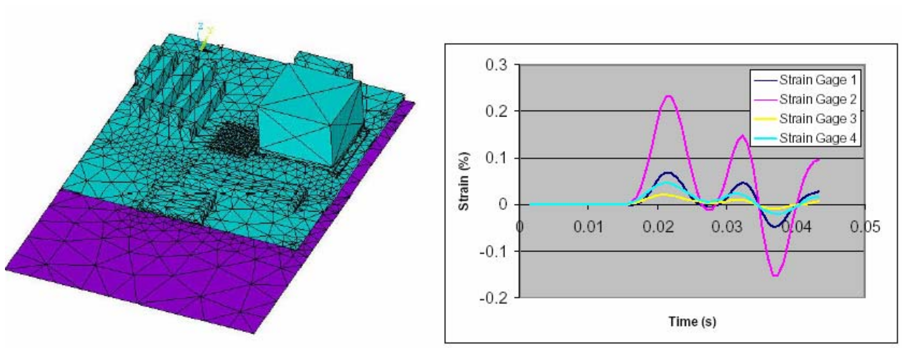

Figure 14 – FEA Simulation of Strain Histories at BGA Corners on PCB Board

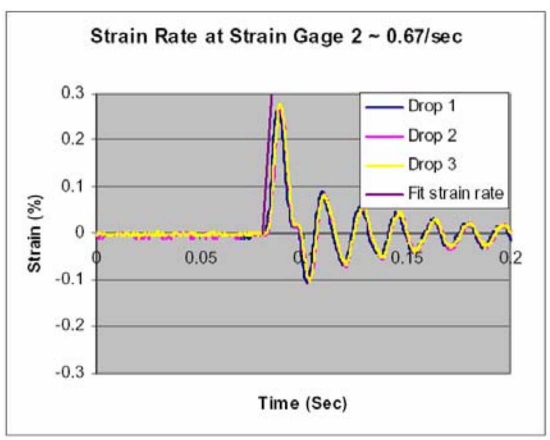

Figure 15 – Strain Response at Strain Gage 2 BGA Corner during Three Shock Pulses – Straight Line: Slope of Strain Rate Range Estimation

Shock with Variable Mass Approach

By mounting an equivalent heat sink mass to a motherboard at the CPU area (Figure 16), a shock test was performed at 50 G acceleration with a trapezoidal pulse and 4.3 m/sec velocity change. Each motherboard is shocked along the three positive and negative directions. Three shocks were performed along each direction. Different masses (450, 600 and 800 grams) were mounted on the motherboard.

Figure 17 shows the board tested in this work. After the shock test, failure analysis (solder joint crosssection) was performed. The test result is summarized:

- • At 450 grams, no discontinuity failure during shock was observed. No solder joint crack was observed.
- • At 600 grams, no discontinuity failure during shock was observed. Very small partial cracks (pad cratering) were observed at the corner joints, as shown in Figure 18.
- • At 800 grams, no discontinuity failure during shock was observed. Also, some boards had memory cards fallen during the shock events. Very small cracks in the PCB under the pads (pad cratering) were observed at the corner joints, as shown in Figure 18.

The variable mass approach provided us a convenient tool for solder joint shock reliability evaluation for thermal mechanical design of heavy mass on boards.

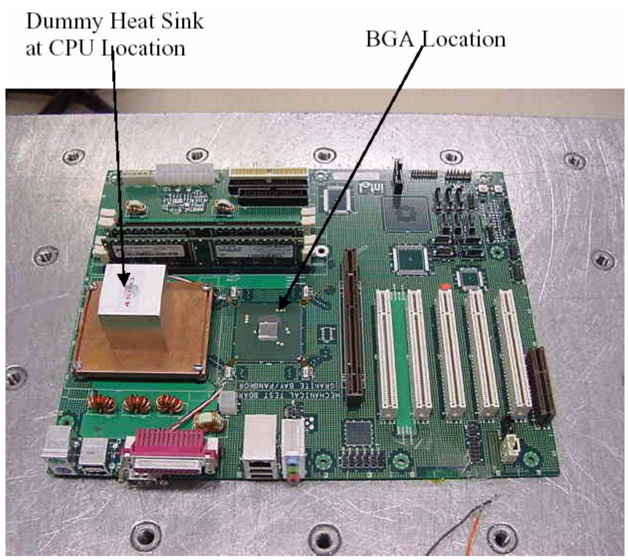

Figure 16 – Shock Test with Variable Mass – An Example of a Typical Mother Board for the Shock Test – Dummy Heat Sink Mounted on CPU Location and the Board is Mounted on a Steel Plate

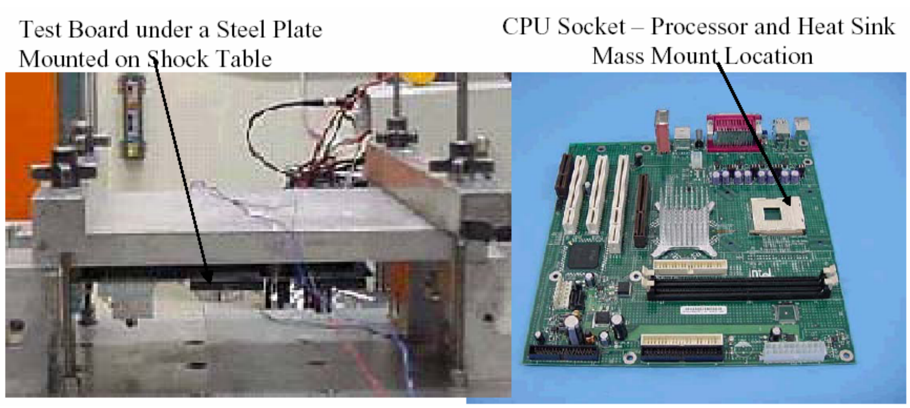

Figure 17 – Test Fixture on a Shock Table and Test Board

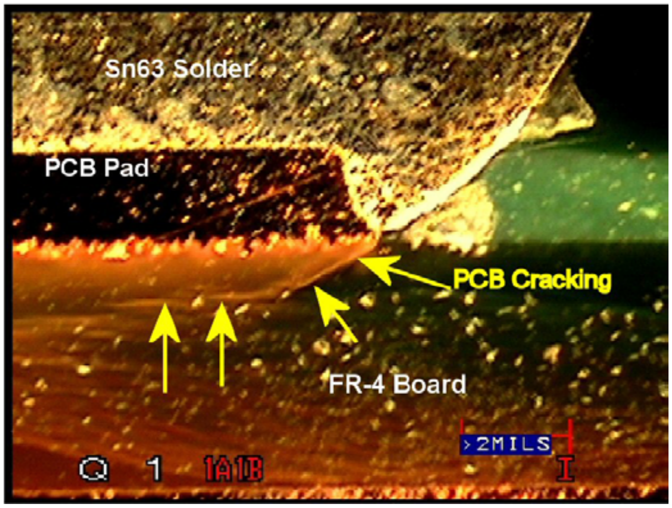

Figure 18 – PCB Crack Under Pad (Micrograph – Dark Field Illumination)

Incremental Shock Test Procedure

In order to evaluate the system failure envelop of a given mass, an incremental shock test procedure was developed to evaluate BGA solder joint shock failures. Repeated shocks at 4.3 m/sec were applied along Z axis (motherboard face down, Figure 19). The first shock is at 35 G, which is a lower bound of a typical product qualification shock level. The G-levels of the first 8~9 shocks were increased by about 10 G sequentially until reaching ~115 G. Afterwards, the shock level stays at ~115 G, as shown in Figure 19. Statistics shows the shock table used has Cpk=1.7 for 50 G within 10% range.

This proposed shock procedure is highly equipment dependent. Some shock table may have different characteristics. By raising the G-level in the first 8~9 shocks, brittle failure (not fatigue failure due to repeated low shock events) may be induced. However, the failure induced may include both brittle fracture and cumulative fatigue fracture, which is more meaningful for real applications. By remaining the same G level after the first 8~9 shocks to accommodate shock table limitation, the focus becomes more on fatigue. Note that this proposed procedure is for large packaged product shock events, not for high G short pulse (e.g. 1700 G with 2 ms sin-pulse) of hand held device.

In-situ solder joint continuity was monitored during the shock events. Through many tests, the monitoring procedure proves solder joint shock failure has a consistent discontinuity fail pattern, as shown in Figure 20. When the first discontinuity was observed during shock #37, further shock #38 showed more joint discontinuity events during the after shock oscillation. This phenomenon progresses with more shocks due to progressive damage.

Tests of motherboards (shown in Figure 17) were performed with the incremental shock procedure and the in-situ solder joint monitoring. Heat sink masses of 450 grams, 600 grams, 800 grams and 1000 grams were used. The number of shocks needed for each board failure is plotted in Figure 21. Heavier heat sink mass clearly results in less shock number to failure. However, one interesting observation is that the failure modes changes from solder joint failure to PCB mounting hole tearing with heavier heat sink. Therefore, the incremental shock test procedure not only provides a failure envelop, but also provides failure mode transition information. Weibull analysis of 450 grams heat sink case showed that 90% motherboard can survive 17+/-9 shocks along z-direction (95% confidence level), which is the 8th shock failure at ~100 G acceleration.

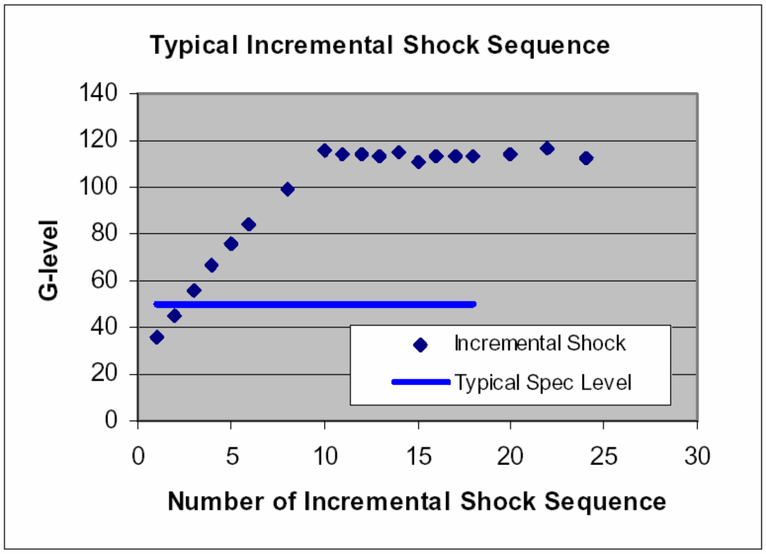

Figure 19 – Incremental Shock Procedure

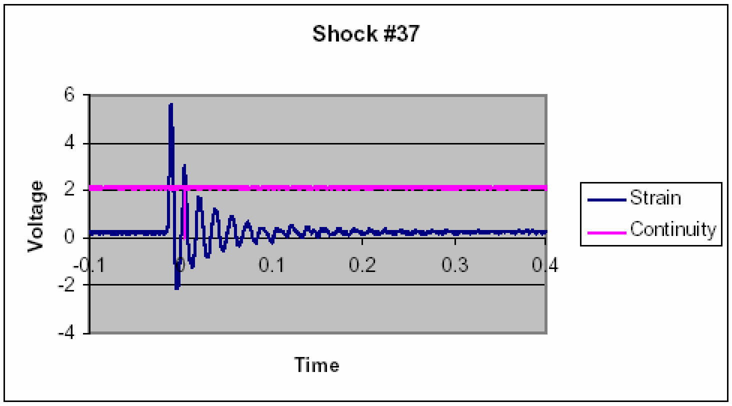

(a) First Discontinuity Event

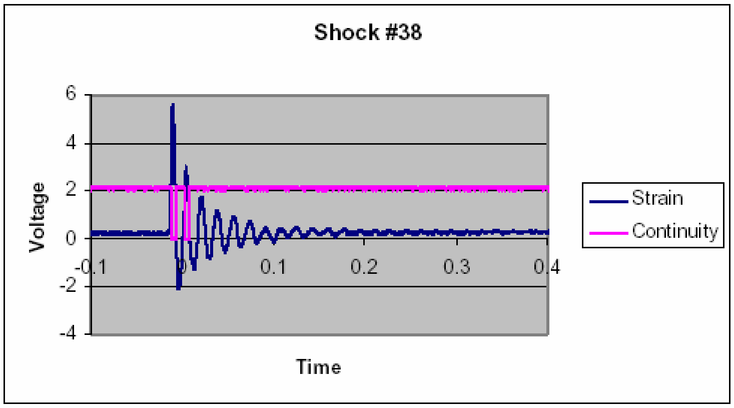

(b) More Discontinuity Events in the Following Shock

Figure 20 –In-situ Solder Joint Shock Monitoring

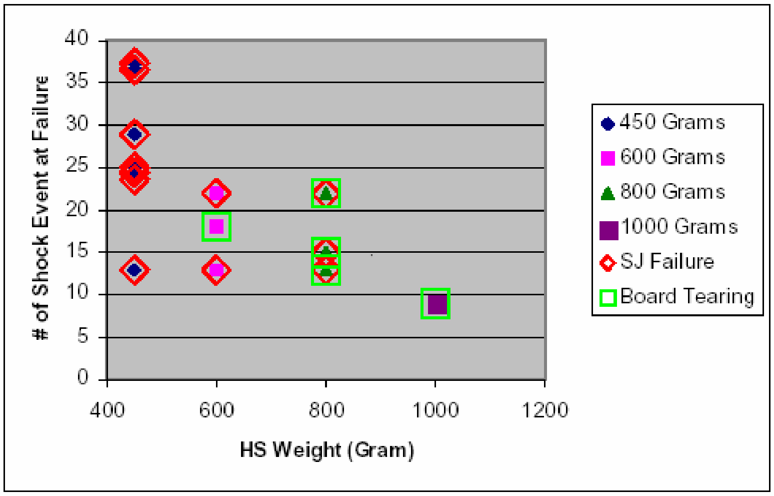

Figure 21 – Number of Shock when Solder Joint Failed

Eight-Point Bend Shock Test

In addition to motherboard shock test, an eight-point bend shock test fixture (Figure 22) was developed similar to those used in the four-point bend test. The loading span (4 inches) is similar to the four-point bend test. In addition to the function of load positioning, a mass is assigned to the loading span fixture for dynamic purpose. The supporting span (8 inches) is mounted to the fixture with six screws (6 points).

In order to achieve similar board response characteristics (fundamental frequency), 96 grams mass is mounted on board through the loading span fixture9. Modal analysis showed that the fundamental (1st resonant frequency) of a motherboard with 450 grams heat sink is close to that of the test coupon with 96 grams of loading span fixture mass.

The test coupon (green board in the figure) is the same as the early four-point bend test with both 45 degree opposite of the loading span mass (Figure 1) and 90 degree (Figure 23) BGA orientations. The BGA is mounted under the PCB board, opposite of the loading span mass.

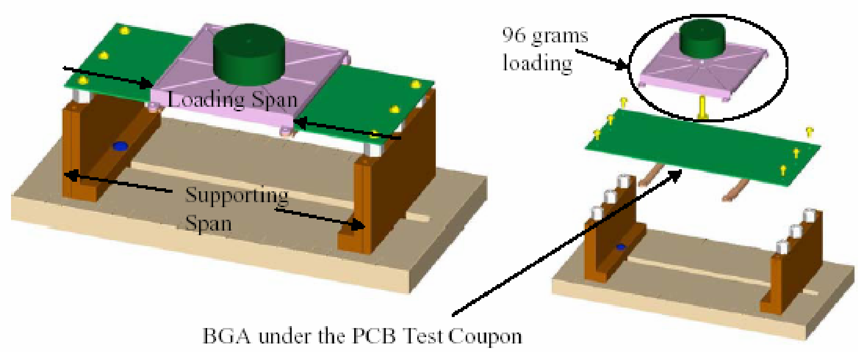

Figure 22 – Eight-Point Bend Shock Fixture

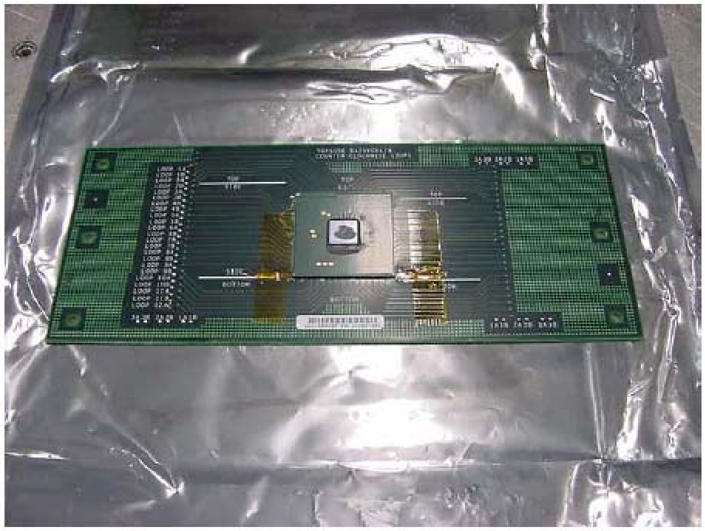

Figure 23 – Test Coupon with 90 Degree BGA Orientation

By using the incremental shock test procedure outlined above, the number of shock to induce solder joint failure, and therefore, acceleration level (G-level) at solder joint failure was obtained, as shown in Figure 24. The mean value and standard deviation of the G-levels are listed in Table 1. BGA orientation at 45 degree failed at lower acceleration level. Both the orientation (exposing corner joint) and the longer equivalent bending length (package diagonal length) may contribute to the lower shock level failure.

With the shock pulse G-level (Table 1) and velocity change (4.3 m/sec) input to the finite element dynamic analysis (Figure 25), the overall behaviors of the test coupon during shock were simulated.

The FEA modal analysis (Table 2) shows that the fundamental frequency of the text fixture/coupon with 96 grams mass is at ~70 Hz, which is typical motherboard responses frequency with 450 grams heat sink mass. The fundamental mode shapes are shown in Figure 26. Detailed discussion of the modal analysis is discussed in the reference[9].

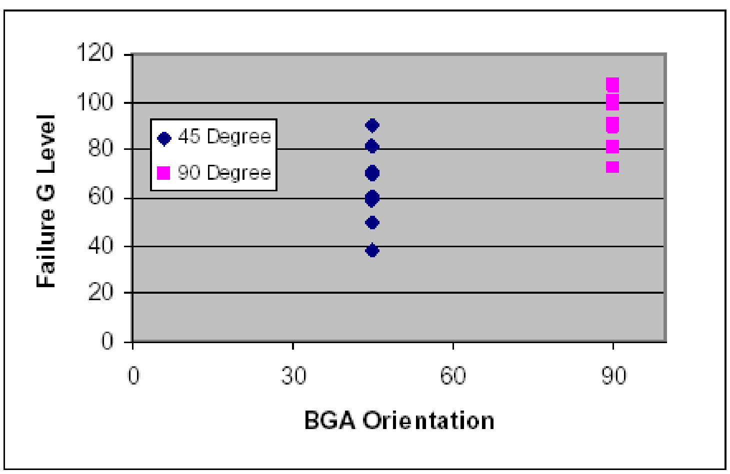

Figure 24 – Failure G Level of Test Coupon with 90 Degree and 45 Degree Orientations

Table 1 – Solder Joint Failure Acceleration Level

Failure G Level	45°	90°
Mean	65 G	93 G
Std Dev	15 G	10 G

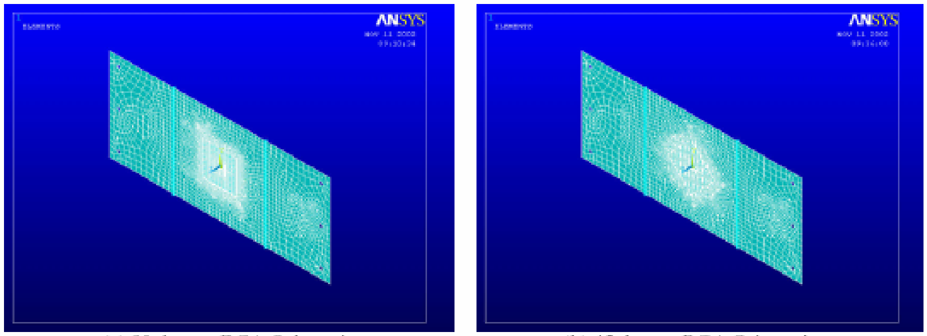

(a) 90 degree BGA Orientation (b) 45 degree BGA Orientation

Figure 25 – Test Coupon Dynamic Finite Element Model

Table 2 – Modal Frequencies at Different Modes

BGA Orientation	90 degree	45 degree
Mode 1	71.4745	71.786
Mode 2	448.642	450.041
Mode 3	478.711	481.528
Mode 4	913.13	922.007
Mode 5	1047.87	1070.31

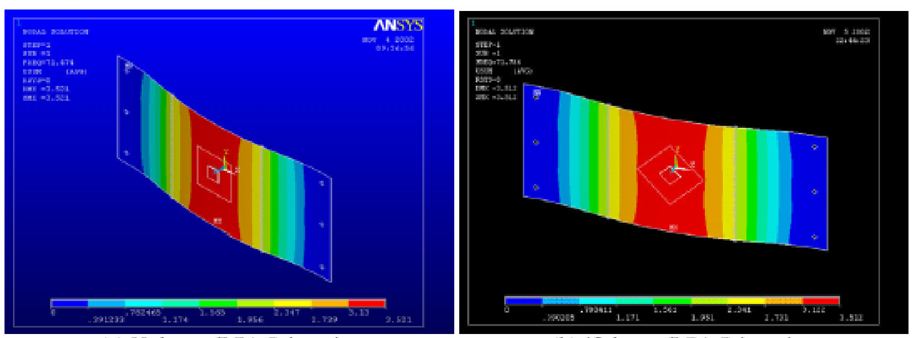

(a) 90 degree BGA Orientation (b) 45 degree BGA Orientation

Figure 26 – Fundamental Mode Shapes

The solder joint force history at the outside row of 90 orientated BGA (Figure 27) was simulated and shown in Figure 28. One can see that for 90 degree BGA orientation, the worst joint is at the corner. The variation of the solder joint failure force of the outside row may not be significant comparing with the failure G-level variation.

The BGA corner joint forces along all three axes are plotted in Figure 29. The transverse shear load along the short axis of the test coupon is negligible, while the longitudinal shear force along the long axis of the test coupon is at the same order of the axial load. The maximum axial load and the corresponding shear load and time are listed in Table 3.

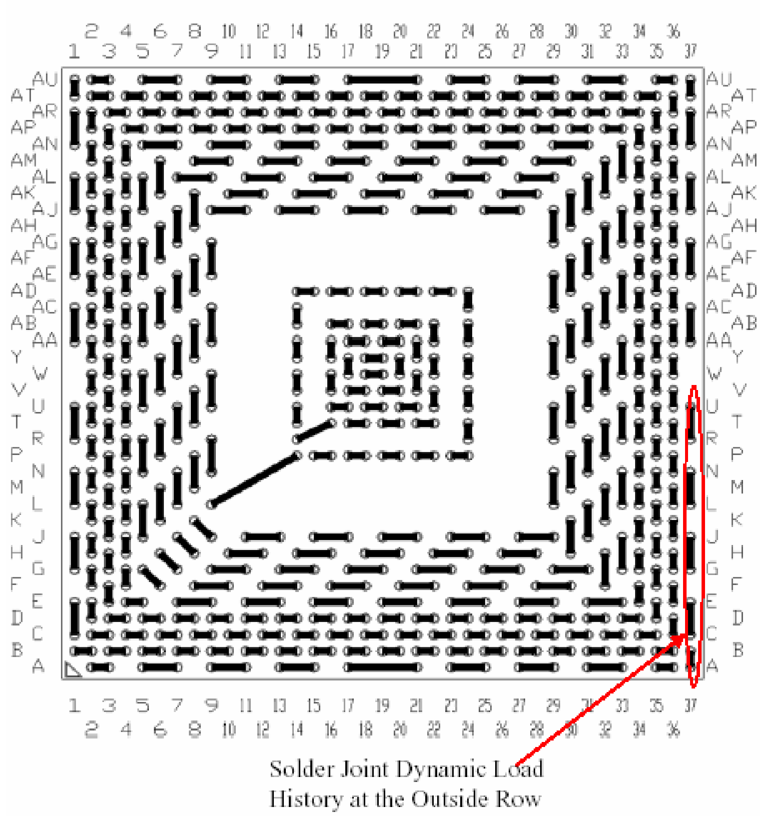

Figure 27 – BGA Ball Pattern

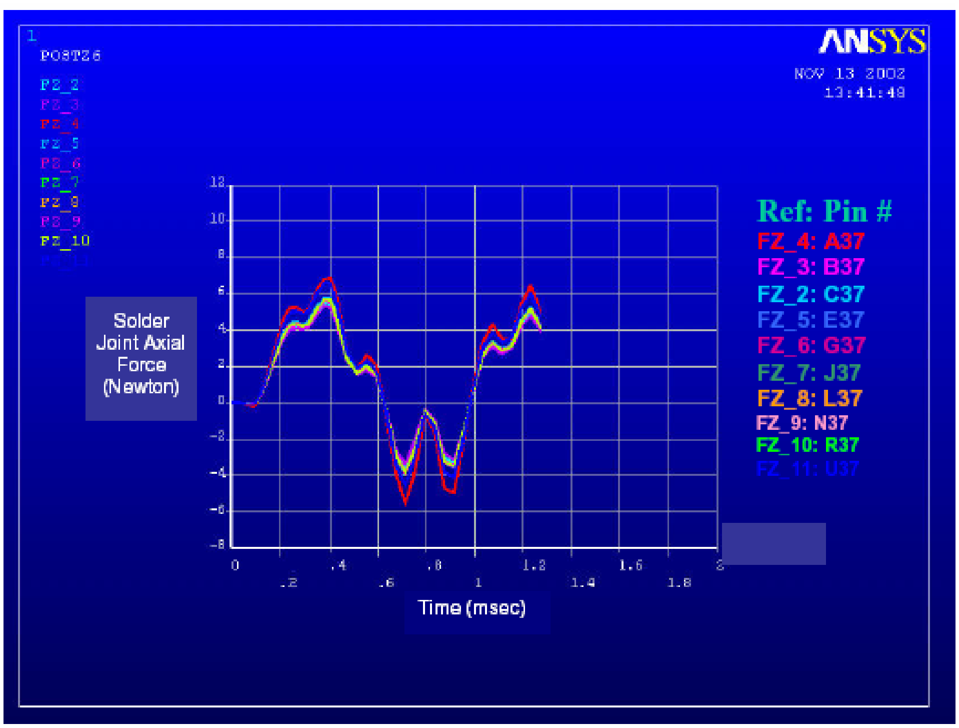

Figure 28 – Solder Joint Axial Load History during Shock

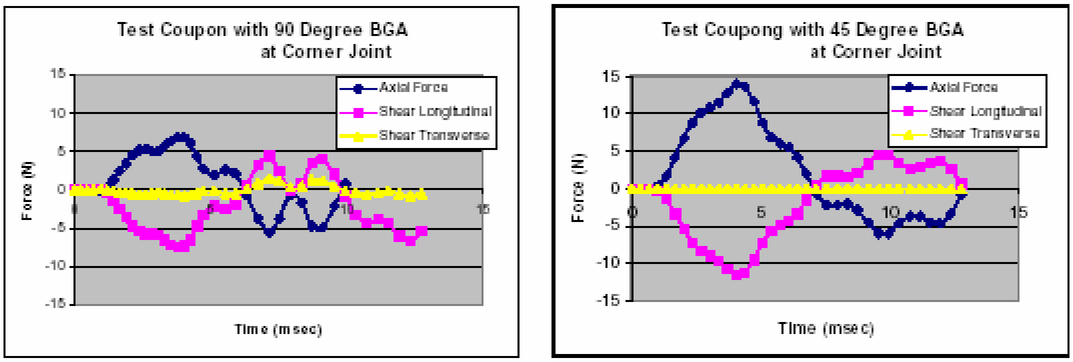

Figure 29 – BGA Corner Solder Joint Load History

Table 3 – Corner Solder Joint Maximum Axial Failure Load Estimation

BGA Orientation	90 degree	45 degree
Max Axial Load	6.87 N	13.96 N (3.1 lbf)
Corresponding Shear (Longitudinal of Test Coupon)	7.40 N (1.7 lbf)	11.58 N (2.6 lbf)
Corresponding Shear (Transverse of Test Coupon)	0.76 N (0.2 lbf)	~0
Corresponding Time	4.02 msec	4.06 msec

At the board level, test coupon with 90 degree BGA failed at higher G-level (Figure 24 and Table 1). While at the solder joint level, the BGA with 90 degree orientation failed at lower axial load. The lower value may be attributed to the fact that the whole solder joint rows of the BGA experienced similar magnitude of dynamic loads (Figure 28) and the weakest one failed first. Therefore, the 90 degree results tend to be the lower bound of solder joint failure load along the outside rows. While for the 45 degree BGA, the corner ball is the only one and the failure load is tend to be the mean value of the corner balls.

When the corner joint load reaches maximal during shock, the maximum principal strain distribution is shown in Figure 30. The highest strain area is the outside rows of the 90 degree BGA and the corner ball of the 45 degree BGA.

Failure analysis of the shocked boards revealed that PCB pad/FR4 failure was the dominant failure mode, as shown in Figure 31. In addition, fracture at IMC between BGA pad and solder ball on the package side was observed.

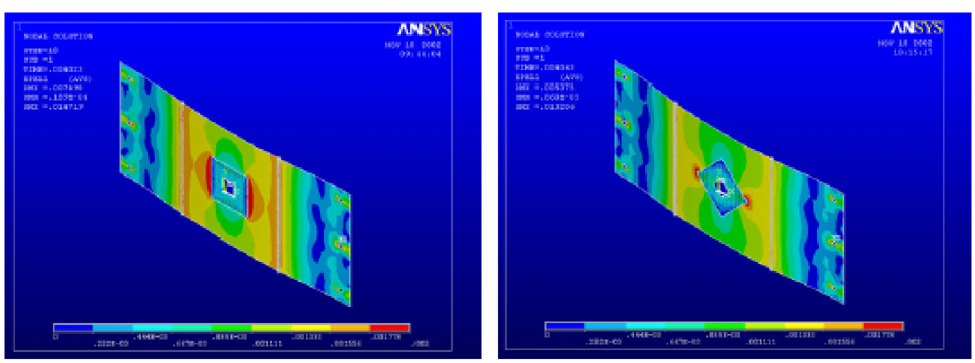

(a) 90 degree BGA Orientation (b) 45 degree BGA Orientation

Figure 30 - Figure 30 – Maximum Principal Strain Distribution when Corner Joint Load Reached Maximum

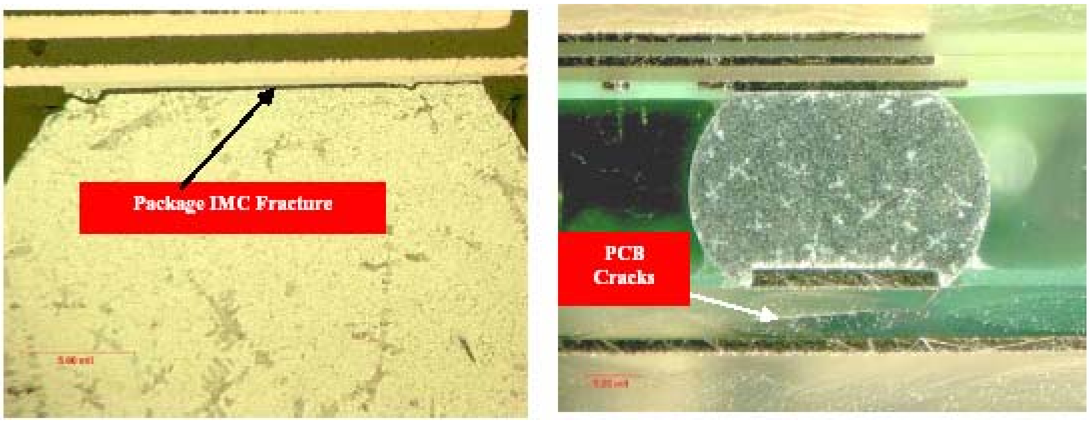

Figure 31 – Cross-Sections of Solder Joint Showing Dominant Failure Modes

Conclusions

1. Solder joint failure is strongly strain rate dependent under flexural load. At higher strain rate, the failure load is lower. The practice of low strain rate (quasi-static) bend test for solder joint failures is not sufficient for dynamic failure prediction due to over-estimation of the joint quasi-static strength.
2. Strain rate under shock load is much higher (0.67/sec in this test) and needs dynamic shock tests to address the solder joint failures.
3. The variable mass approach provides a convenient way for shock failure modes and envelop evaluation at a given shock level.
4. The incremental shock test procedure provides not only shock failure envelops, but also shock failure mode transition at different heat sink mass. The in-situ shock monitoring shows the characteristics of solder joint discontinuity under repeated shock events. However, the higher shock acceleration level may result in different failure modes not relevant to the usage conditions.
5. The eight-point bend shock test and modeling provided the solder joint level failure force. This failure force is a valuable input for solder joint reliability modeling. In summary, various test and modeling methodologies were explored for solder joint reliability evaluation under dynamic load. The applicability of these test methods were discussed and recommended for design and reliability evaluations.

References

1. Geng, P, "Solder Joint Shock Testing and Modeling Methodology Development," *IPC Annual Conference*, IPC 6-10d Committee Meeting, Minneapolis, MN, September. 2003
2. Pitarresi, J, P. Geng, W. M. Beltman, and Y. Ling, "Dynamic Modeling and Measurement of Personal Computer Motherboard," *Proc 52nd Electronic Components and Technology Conf*, San Diego, CA, May. 2002
3. Shi, X.Q. *et al*, "Effect of Temperature and Strain Rate on Mechanical Properties of 63Sn/37Pb Solder Alloy," Journal of Electronic Packaging, Vol. 121, (1995) pp. 179-185
4. Dai, L.H. and Lee, S-W R., "Characterization of Strain Rate-Dependent Behavior of 63Sn-37Pb Solder Alloy," *Proc of IPACK'01—The Pacific Rim/ASME International Electronic Packaging Technical Conference and Exhibition*, Kauai, Hawaii, July 2001
5. Geng, P, P. H. Chen, and Y. Ling, "Effect of Strain Rate on Solder Joint Failure under Mechanical Load," *Proc 52nd Electronic Components and Technology Conf*, San Diego, CA, May. Pp. 974-978, 2002
6. Goyal. D, T. Lane, P. Kinzie, C. Panichas, K. M. Chong and O. Villalobos, "Failure Mechanism of Brittle Solder joint Fracture in the Presence of Electroless Nickel Immersion Gold (ENIG) Interface," *Proc 52nd Electronic Components and Technology Conf*, San Diego, CA, May. Pp. 732-739, 2002
7. Harada, K, S. Baba, Q. Wu, H. Matsushima, T. Matsunaga, Y. Uegai, and M. Kimura, "Analysis of Solder Joint Fracture under Mechanical Bending Test," *Proc 53rd Electronic Components and Technology Conf*, New Orleans, LA, May. 2003
8. Geng, P. and W. M. Beltman, "Monitoring Motherboard Shock Response near BGA Solder Joints," *Proc SMTA International Conf*, Chicago, IL, September, 2002
9. Geng, P., W. M. Beltman, P. H. Chen, G. Daskalakis, D. Shia and M. H. Williams "Modal Analysis for BGA Shock Test Board and Fixture Design," *Proc IEEE CPTM*, Singapore, December, 2003

Acknowledgement
The first author wishes to thank Tom Worley, Mike Lane, Bill Bader, Yun Ling, Yinan Wu, Murli Tirumala and Martin Rausch at Intel for their generous technical and financial support of this project. Thanks to Werner Engelmaier and Dr. Reza Ghaffarian for their leadership at IPC. We would like to acknowledge Norman Armendariz, Marco Beltman, Karissa Blue, Philip H. Chen, George Daskalakis, Michael Reynolds, Pete Robson, David Shia, Guixiang Tan, Michael H. Williams and many of our colleagues at Intel for their contribution to this project. The work of Randall Durand, Eric Salskov and Dan Tong is gratefully acknowledged.